Quaternary Science Reviews 373 (2026) 109714

Contents lists available at ScienceDirect

Quaternary Science Reviews

journal homepage: www.elsevier.com/locate/quascirev

Climate change and hominin behavioral adaptations during the Marine Isotope Stage 5 to 4 transition: a case study from Donggou site, Nihewan Basin, North China

Jingyue Xu[a,b,c], Dongwei Niu[d,e,*], Shengrui Zhang[f], Yujie Guo[d,e], Xiaoli Li[g], Shuwen Pei[a,b,**]

[a] Key Laboratory of Vertebrate Evolution and Human Origins, Institute of Vertebrate Paleontology and Paleoanthropology, Chinese Academy of Sciences, Beijing, 100044, China
[b] Key Scientific Research Base on Paleolithic Human Evolution and Paleogenetics (IVPP), SACH, Beijing, 100044, China
[c] University of Chinese Academy of Sciences, Beijing, 100049, China
[d] College of History and Culture, Hebei Normal University, Shijiazhuang, Hebei, 050024, China
[e] Hebei Key Laboratory of East Asian Human Origin and Civilization Research, Hebei Normal University, Shijiazhuang, 050024, China
[f] School of Geographical Sciences, Hebei Normal University, Shijiazhuang, Hebei, 050024, China
[g] National Natural History Museum of China, Beijing, 100050, China

ARTICLE INFO

Handling editor: Claude Hillaire-Marcel

Keywords:
Marine Isotope Stage (MIS) 5 to 4 transition
Climate and environmental variations
Hominin adaptation
Donggou site
Nihewan Basin
North China

ABSTRACT

The transition from Marine Isotope Stage (MIS) 5 to MIS 4 was a major climatic shift that affected hominin biological and cultural evolution in eastern Eurasia. Marked by abrupt climatic shifts, this stage is characterized by notable diversification in hominin behavior. Technological and behavioral changes co-occurred with fluctuating ecological regimes, coinciding with the transition of millennial-scale climate events at the terminus of MIS 5, forcing hominins to develop new strategies to exploit their environment. Temporal multi-proxy-based climate and environmental reconstructions from the Donggou site in the Nihewan Basin of North China offer a high-resolution archive of climatic variation for this period, providing insights into its impact on hominin adaptive strategies. Luminescence dating indicates that the Donggou site was formed between 126.1 and 70.1 ka, and hominins occupied the site from 76 to 74ka. Our results suggest that the regional climate was colder and drier than today and underwent frequent climatic fluctuations that drove environmental and landscape changes. The Donggou hominins persisted in the initial arid phase. They continued to occupy the river floodplain landscape during the mild and moist Dansgaard-Oeschger event of late MIS 5a, before the climate deterioration of the MIS 4 episode. The Donggou archaeological data revealed flexible adaptive strategies, including the effective use of high-quality lithic raw materials, an increase in retouched tools, systematic exploitation of ungulates, and the use of fire. Other sites in the region exhibited different adaptive strategies, collectively indicating hominin behavioral diversification during this period. We suggest that climate oscillation during the MIS 5–4 transition may have promoted hominins to adjust their strategies and develop solutions to challenging environments, leading to increased behavioral flexibility and capabilities when facing landscape turnover from lakeshore to river floodplain habitats after the Nihewan Old Lake dies out.

1. Introduction

Studies on the relationship between environmental change and human evolution have focused on temporal correlations between global and regional climate fluctuations, and major human evolutionary events (Potts, 2012, 2013; Sandweiss and Kelley, 2012; Grove, 2014; Potts et al., 2018; Ruan et al., 2023; Timmermann, 2020; Xu et al., 2023; Zan et al., 2024). The early part of the Late Pleistocene (known as Marine Isotope Stages (MIS)5 to 4), characterized by a critical climate shift, witnessed a substantial transition from warm interglacial to cold glacial periods in the Earth's climate (Blunier and Brook, 2001; Hemming, 2004; Wang et al., 2008a; Yang and Ding, 2014; Cheng et al., 2016).

* Corresponding author. College of History and Culture, Hebei Normal University. Shijiazhuang, Hebei, 050024, China.
** Corresponding author. Key Laboratory of Vertebrate Evolution and Human Origins, Institute of Vertebrate Paleontology and Paleoanthropology, Chinese Academy of Sciences, Beijing, 100044, China.
E-mail addresses: ndw1986@163.com (D. Niu), peishuwen@ivpp.ac.cn (S. Pei).

https://doi.org/10.1016/j.quascirev.2025.109714
Received 7 July 2025; Received in revised form 15 November 2025; Accepted 15 November 2025
Available online 3 December 2025

Such climate fluctuations have a profound influence on hominin adaptation across East Asian landmasses (deMenocal and Stringer, 2016; Timmermann and Friedrich, 2016; Bae, 2017; Bae et al., 2017; Ao et al., 2024). Recent studies indicate that the initial dispersal of modern humans, or *Homo sapiens*, from their African homeland to remote East Asia most likely occurred during the last interglacial episode (MIS 5) in the southern and subtropical regions of China (Liu et al., 2010a, 2010b, 2015; Bae et al., 2014, 2018; Ao et al., 2024). In contrast, available hominin fossils (Tong et al., 2004; Shang et al., 2007), dates (Li et al., 2018, 2019a; Wang et al., 2022; Yang et al., 2024), ancient DNA (Fu et al., 2013), and Initial Upper Paleolithic and Upper Paleolithic archaeological evidence (Kuhn, 2019; Wang et al., 2022; Yang et al., 2024; Zwyns, 2021) indicate that *H. sapiens* spread eastward across northern Asia to North China between 50 ka and 40 ka during MIS 3 (Bae, 2017, 2024a, 2024b; Li et al., 2019b, 2020; Li, 2024). However, it remains unclear whether behavioral flexibility and technological innovations enabled hominins to withstand MIS 5–4 climatic oscillations before the dispersal of modern humans in North China. To address these questions, multi-proxy climate and environmental datasets combined with archaeological evidence from archaeo-stratigraphic sequences with precise ages, are vital for exploring the hominin behavioral patterns and adaptations during climate and ecological variations.

The Nihewan Basin is a crucial center for investigating hominin adaptation to environmental changes in East Asia, particularly in North China (Yang et al., 2020; Pei et al., 2024). The long and well-preserved fluvial-lacustrine sediments (known as the Nihewan Beds (Barbour, 1924) in the region are rich in well-preserved Paleolithic sites from the Early Pleistocene to the late Middle Pleistocene (Wei and Xie, 1989; Xie et al., 2006; Keates, 2010; Wang and Sun, 2023; Pei et al., 2024). Current research on how climatic fluctuations affect hominin adaptation is derived from lakeshore environments, which indicates that environmental fluctuations may have driven flexibility and innovations in various aspects of technological behaviors and allowed hominins to face the ecological challenges of northern middle to high latitudes during the formation of the fluvial-lacustrine sequence (Li et al., 2016; Pei et al., 2019; Yang et al., 2017, 2021; Xu et al., 2021, 2023). Along with the demise of the Nihewan paleolake (Zhao et al., 2010; Guo et al., 2016; Deng et al., 2019), the Late Pleistocene witnessed fluvio-lacustrine deposits that underwent significant erosion, leading to a shift in landscape from the lake shore to the alluvial environment. The wide spread landscapes of fluvial deposits from river terraces and capped loess from the last interglacial to glacial episodes provide opportunities to decipher how climate and environmental fluctuations affect hominin adaptive strategies. However, the adaptability of hominin behavior in this setting remains unclear, hindering the exploration of hominin dispersal and behavioral adaptation in North China.

The Donggou site (DG) is an important site located within the fluvial river terrace of the Yuxian sub-basin, one of the three sub-basins of the Nihewan Basin (Pei et al., 2024; Ye et al., 2024) (Fig. 1a and b). Archaeological evidence indicates a relatively long-distance transportation of exotic high-quality lithic raw materials, increased refinement of retouched tools, systematic exploitation of ungulates, and even the use of fire, indicative of hominin behavioral flexibility (Zhou et al., 2024; Xu et al., 2024). The well-preserved stratigraphic sequence of river terraces, overlain by loess from the last interglacial and glacial periods, provides a suitable basis for dating and environmental reconstruction in the region. In this study, we discussed the results of paleoenvironmental reconstructions based on well-constructed optically stimulated luminescence (OSL) dates, organic carbon isotopes ($\delta^{13}C_{org}$) analyses, pollen analyses, and mean annual precipitation (MAP) reconstruction analyses of the DG archaeo-stratigraphic sequence. By combining our results with evidence of behavioral strategies, we aimed to contextualize climate and environmental variability during the MIS 5 to 4 transition. This approach provides a perspective on the adaptive strategies and behavioral transformations of hominins at the Donggou site and across the Nihewan Basin.

2. Regional setting

The Nihewan Basin (39° 33′–40° 22′ N, 114° 25′–115° 31′ E), located

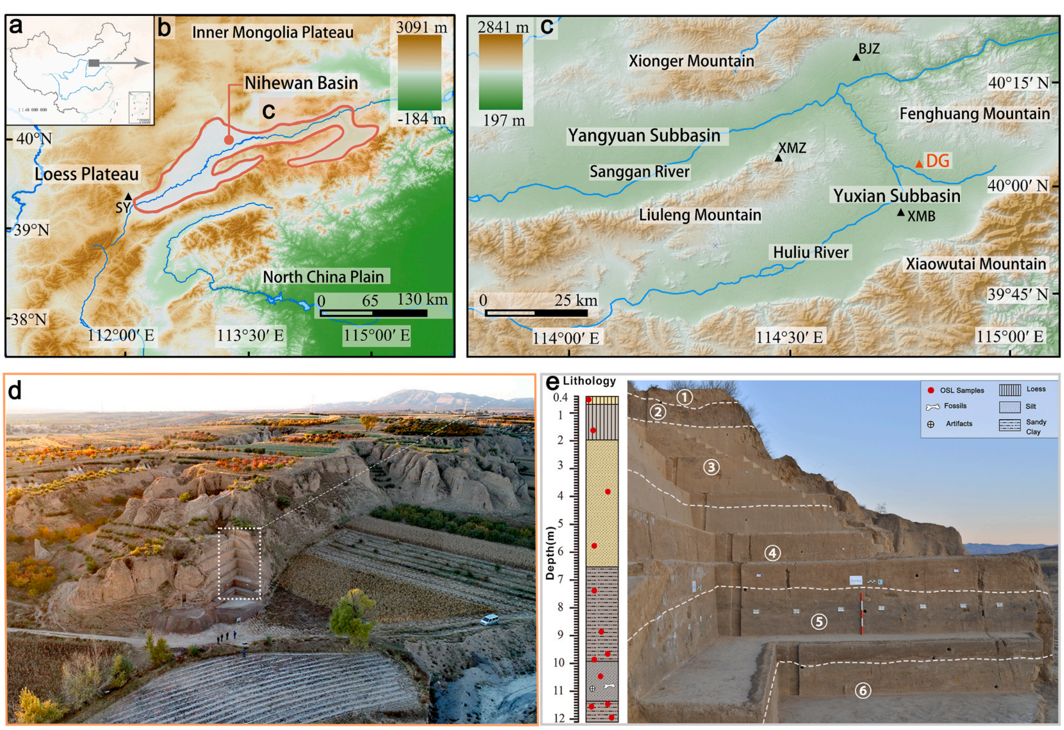

Fig. 1. Geographical and geological background of the Donggou site in the Nihewan Basin. a-b. Location of the Nihewan Basin and Shiyu site (SY); c. Location of the Donggou (DG) site and other relevant sites (BJZ: Banjingzi; XMZ: Xinmiaozhuang; XMB: Xiamabei) in the Nihewan Basin; d. Landscape and excavated area of Donggou site; e. Stratigraphic sequence of Donggou site.

on the eastern margin of the Loess Plateau at the junction with the Inner Mongolian Plateau and North China Plain at a latitude of approximately 40° N, is an important center of successive hominin settlements in North China (Fig. 1a-b) (Yang et al., 2020; Pei et al., 2024). The Nihewan paleolake began to develop during the Late Pliocene (Ao et al., 2013; Deng et al., 2019) and was infilled with a thick sequence of Pliocene-Pleistocene fluvio-lacustrine deposits. Because of the elevation of the block and intensification of erosion, the lake finally vanished in the late Mid-Pleistocene, leading to the formation of an alluvial river network during the Late Pleistocene (Xia and Liu, 1984; Zhou et al., 1991).

The Nihewan Basin is located in the transitional zone between warm-temperate, semi-humid, and semi-arid climates (Yuan et al., 2011). Spring is characterized by dry and windy conditions with an extensive temperature range, and where substantial aeolian sand transport occurs. Summer is characterized by high temperatures and rainfall accounts for 62–67 % of the annual total precipitation. Autumn is cool and humid, and winter is cold and long. The regional mean yearly temperature ranges from 7.4 to 9.6 °C and MAP ranges from 224 to 593 mm (Yuan et al., 2011; Zhou et al., 1991).

The natural regional vegetation of the Nihewan Basin ranges from warm-temperate deciduous broad-leaved forests to temperate semi-arid steppes (Lu et al., 2018). The surrounding mountains contain natural secondary and planted forests dominated by *Betula*, *Populus*, *Quercus*, *Pinus tabulaeformis*, and *Larix principis-rupprechtii*. The semi-arid and arid shrublands are dominated by *Caragana microphylla*, *Vitex negundo* var. *heterophylla*, *Zizipus jujuba* var. *spinosa*, *Hippophae rhamnoides*, *Bothriochloa ischaemum*, and *Artemisia gmelinii*, which are widely distributed on the lower hills. Most river valleys are cultivated with crops such as *Zea mays*, *Sorghum vulgare*, *Setaria italica*, and others (Yuan et al., 2011).

3. Materials and methods

3.1. Stratigraphy and samples

The DG site (40° 02′ 51.0″ N, 114° 48′ 09.6″ E, elevation 905 m) is located on the right bank of the DG tributary of the Ding'an River (a tributary of the Huliu River) in the eastern part of the Yuxian sub-basin (Fig. 1c and d). The Nihewan paleo-lake deposits were dissected by numerous streams originating from the northern mountains, leading to the formation of a DG tributary river terrace in this area. The DG site is buried in the lower part of the second terrace. In the DG, the exposed profile is more than 14 m thick and consists mainly of greyish lacustrine deposits, dark grey gravel layers, greyish-yellow and greyish-black silty clays, silts, and sands, which are capped by loess. The stratigraphic sequence was eroded and cut by modern DG streams originating in the northern mountainous region, resulting in small valleys interspersed throughout the sequence and shaping the contemporary landscape (Fig. 1d). The DG archaeo-stratigraphic sequence comprises 1.0 m of a river bed unit, and 10 m of a river floodplain unit, overlain by 2.0 m of loess deposits, and can be divided into six layers (Fig. 1e; Supplementary Material, Table SM1) (Zhou et al., 2024). Archaeological remains were unearthed from silts and fine sands, with depths from 9.9 m to 11.4 m corresponding to past river floodplain environments (Fig. 1e). Low levels of abrasion and spatial analysis indicated that the bone and stone tools were not transported over long distances, suggesting that they were most likely buried *in situ* (Xu et al., 2024).

A total of 145 environmental samples were systematically collected at 10 cm intervals (5 cm intervals within the archaeological layer) from 0.4 to 12.0 m of the archaeo-stratigraphic sequence of the DG site (depths of 0–0.4 m was excluded from further analyses due to modern human disturbance). All samples were used for integrated analyses of pollen and organic carbon isotope ratios.

3.2. Archaeology

The DG site was discovered and identified in 2017 and an excavation in the same year covered a total area of 25 m^2 (Fig. 1d). The DG lithic assemblage consists of 2892 artifacts, which were classified into freehand-made cores (n = 77, 3.79 %), retouched tools (n = 110, 5.42 %), detached pieces (n = 1828, 90.05 %), bipolars (n = 11, 0.54 %), and pounded artifacts (n = 4, 0.20 %) (Zhou et al., 2024) (Fig. 2a–m). DG knappers intentionally procured raw materials from local river-beds and employed core and flake technologies in North China. However, evidence of the transport of high-quality materials such as chalcedony, opal, and agate, an increased number of retouched tools (Fig. 2), and the use of freehand and bipolar techniques in alternative contexts show that hominins at the site adopted technological flexibility.

In addition, the DG archaeological layers preserved 7146 fossil fragments, including those of Rodentia, *Meles*, *Coelodonta*, *Equus*, *Cervus*, and Bovidae, with *Cervus* and Bovidae dominating the faunal assemblage (He, 2025). Preliminary studies have shown that animal bones from the DG site are preserved in near-primary condition after prolonged exposure to air, indicating that hominins had primary access to animal carcasses. The construction of body part profiles for the main animal species from the DG noted a trend toward selective transport of animal parts at the site. The presence of cut marks indicates various subsistence activities once undertaken by hominins at the site, such as skinning, dismembering, and defleshing (Fig. 2n–p). Percussion traces (Fig. 2n) registered on animal bones indicate the marrow extraction strategies of the DG inhabitants. Moreover, 20 percent of the bones were burnt, and some were even highly carbonized (Fig. 2p), suggesting the possible use of fire at the DG site, as further evidenced by hearths and burnt stones. Carnivores and rodents may subsequently scavenge the remaining parts of the animals (He, 2025).

3.3. OSL dating and chronology

Twelve sediment samples, named 23DG-OSL-1, -2 and 17DG-OSL-03 to −12 from top to bottom, were systematically collected from the excavated sedimentary profile (Fig. 1e) and then tested with the OSL method at Hebei Normal University (Huang et al., 2025). Sample 23DG-OSL-1 was collected from the top modern aeolian deposits behind the excavation profile; sample 23DG-OSL-2 from Layer 2; samples 17DG-OSL-03 and -04 from Layer 3; samples 17DG-OSL-05, -06, and −07 from Layer 4; 17DG-OSL-08 and -09 from Layer 5; and samples 17DG-OSL-10, -11, and −12 from Layer 6. Cultural remains were mainly recovered from Layer 5. The single-aliquot and single-grain MET-pIRIR$_{50–250°C}$ (multiple elevated temperatures post-infrared infrared stimulated luminescence) dating method was used on K-feldspar grains for testing (measurement details in Huang et al., 2025).

3.4. Environmental reconstruction

3.4.1. Stable carbon isotope ($\delta^{13}C_{org}$) analysis

All environmental samples were used to analyze the stable carbon isotope of organic matter ($\delta^{13}C_{org}$). After thorough drying, the samples were ground with a mortar and pestle and passed through a 200-mesh (75 μm) sieve. To remove the carbonates, approximately 1.5g of the sieved sample was treated with 2 mol/L HCl for 24 h. The samples were then rinsed with deionized water to neutral pH and oven-dried. Approximately 20 mg of the treated samples was weighed for carbon isotope analysis. The $\delta^{13}C$ values of the samples were measured using a Flash2000HT elemental analyzer interfaced to a 253 Plus continuous-flow isotope-ratio mass spectrometer (IRMS). Standard reference materials were Urea#1 ($\delta^{13}C$ = −34.1 ‰ VPDB), Urea#2 ($\delta^{13}C$ = −8.0 ‰ VPDB), Urea#3 ($\delta^{13}C$ = 11.7 ‰ VPDB), and an international isotope reference material (IAEA-CH3; $\delta^{13}C$ = −24.7 ‰ VPDB) were used to assess the analytical accuracy of the EA-IRMS. The standard deviation for repeated measurements of $\delta^{13}C$ is $< \pm 0.2$ ‰ (Wang et al., 2023). The

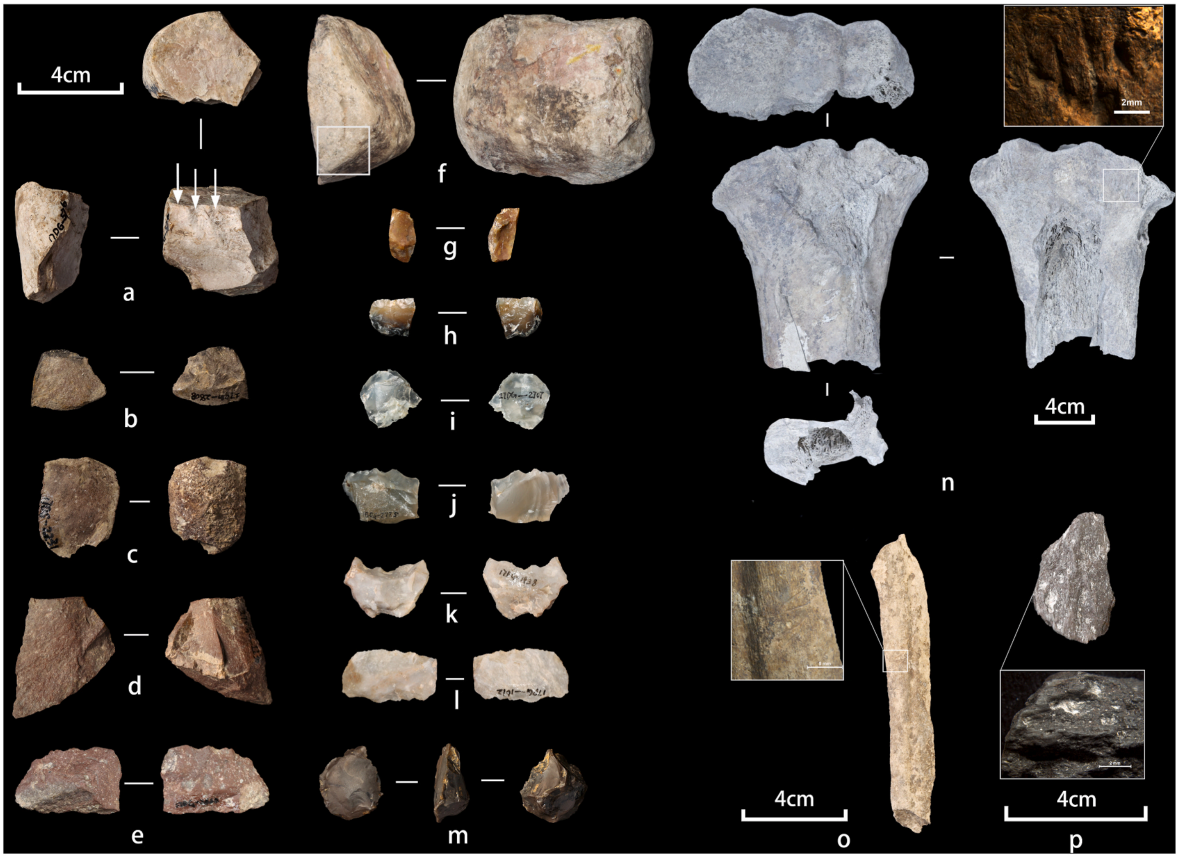

Fig. 2. Selected remains from the Donggou site. a: core; b, c, d, i: flakes; g: bipolar flake; e, h, j, k, l: scrapers; m: point; f: stone hammer; n: broken right radius of Bovidae with percussion marks; o: metacarpal bone of Bovidae with cut marks; p: burnt bone.

pretreatment experiment and stable carbon isotopes data analysis in this study were conducted at the Institute of Vertebrate Paleontology and Paleoanthropology, Chinese Academy of Sciences.

3.4.2. *Pollen analysis processing*

Pollen grains were concentrated from dried sediments with a modified HCl-NaOH-HF treatment, and then sieved and floated by heavy liquid, progressively increasing the sample weight and number of flotation for the same batch of samples (Faegri et al., 2000). To calculate pollen concentration, one tablet of *Lycopodium* spores (10,315 ± 200 grains) was added to each sample before pretreatment. The extracted pollen was identified and examined under a Leica DM5500B microscope (400–600 × magnification) using *The Pollen Flora of China* (Wang, 1995) and *Atlas of Quaternary Pollen and Spores in China* (Tang et al., 2020). Approximately 300 terrestrial pollen grains were counted in each sample. Pollen percentages and concentrations were calculated according to the method described by Zhang et al. (2020). The pollen percentages of terrestrial plants were based on the sum of the total terrestrial pollen grains. In contrast, the percentages of aquatic pollen types and fern spores were based on the sum of the terrestrial pollen grains, aquatic pollen grains, and fern spores. The pollen experiments and analyses were performed at the Environmental Archaeology Laboratory of Hebei Normal University. Tilia (version 3.0.2) was used for data processing and plotting (Grimm, 2019).

3.4.3. *Quantitative climate reconstruction*

As one of the most widely used methods for quantitative paleoclimatic reconstruction, weighted averaging partial least squares (WAPLS) regression has been used to establish a transfer function between modern pollen assemblages and climatic parameters (Zhang et al., 2022a). In this study, we reconstructed MAP using a pollen transfer model based on WAPLS. The model performance was assessed using the leave-one-out cross-validation method (Birks et al., 2012). Modern pollen data were obtained from Cao et al. (2014). The climatic data for modern surface pollen samples were extracted from the WorldClim database (Fick and Hijmans, 2017). All analyses were performed in R (version 4.4.2) using the "rioja" package (Juggins, 2009).

4. Results

4.1. *Chronology of the DG site*

The environmental dose rate, De, measured age, and Bayesian modelled age values for each sample are summarized (see Supplementary Material, Table SM2). The modelled ages were consistent with the measured OSL ages. They conformed to the stratigraphic order, supporting the robustness of the dating results (Fig. 3). The modelled results indicated that the 6th layer of the site was dated to approximately 126.1–98.4 ka. A depositional discontinuity of ~23 ka was observed between the 6th and 5th layers, although no obvious erosional surface was observed during the field investigation, suggesting limited fluvial or eolian reworking. A marked increase in sediment accumulation was observed between Layers 5 and 3, dated from ~75.9 to ~71.5 ka. From the second layer (~71.5 ka) onward, the fluvial terrace development ceased, leading to aeolian deposition. The archaeological layer is bracketed between 75.9 ± 5.2 ka and 73.6 ± 3.0 ka, indicating hominin occupation around 76 to 74 ka.

4.2. *$\delta^{13}C_{org}$ values*

The $\delta^{13}C_{org}$ values of the DG archaeo-stratigraphic sequence are shown in Fig. 4, ranging from −24.7 ‰ to −16.7 ‰, with an average of

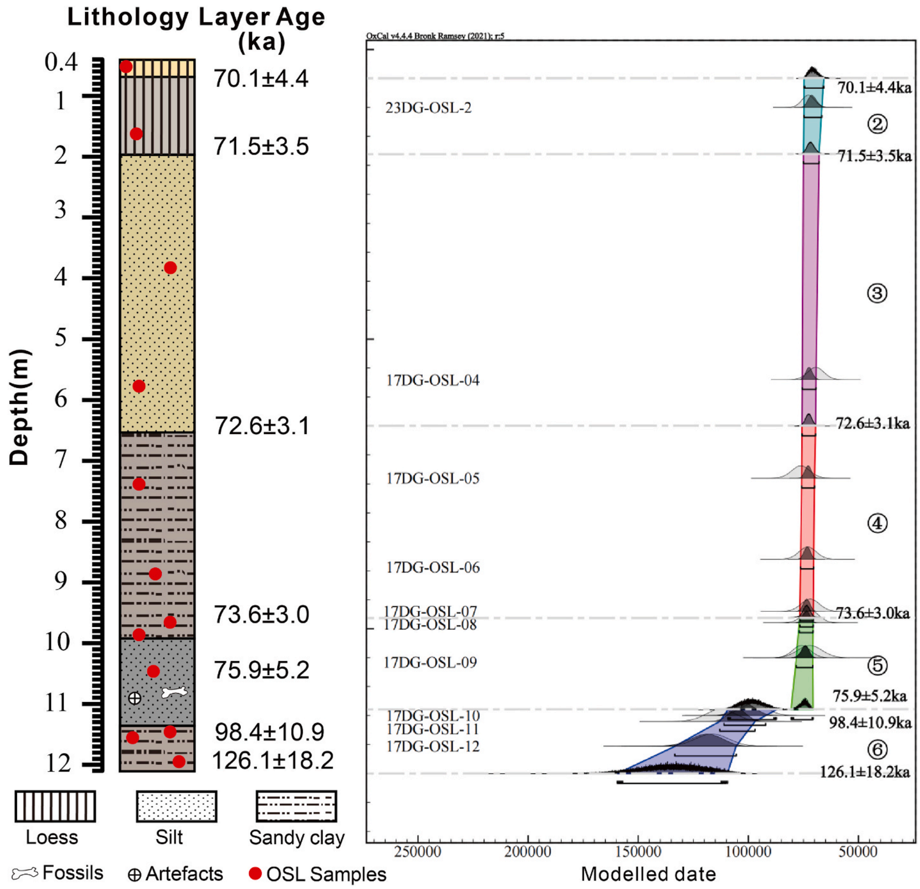

Fig. 3. Age-depth model of Donggou archaeo-stratigraphic sequence (②~⑥represent stratigraphic layers) (modified after Huang et al., 2025).

−21.7 ‰. In Layer 6 (from 1215 cm to 1135 cm), the $\delta^{13}C_{org}$ values are relatively positive, fluctuating between −23.1 ‰ and −20.5 ‰ (average value of −21.6 ‰). During the period of hominin occupation (corresponding to the accumulation of Layer 5), the $\delta^{13}C_{org}$ values present a negative but fluctuating trend compared with the previous stage, varying from −24.6 ‰ to −19.0 ‰ (average on−22.5 ‰), reaching a peak of −19 ‰. The $\delta^{13}C_{org}$ increases gradually in Layers 4 and 3 from −24.1 ‰ to −16.7 ‰, with an average of −21.2 ‰. Two notable positive fluctuations were observed at 750 cm (−18 ‰) and at the depth of 700–580 cm, after which the $\delta^{13}C_{org}$ exhibited a gradual increase. In the loess accumulation (Layer 2–1), $\delta^{13}C_{org}$ values showed a negative trend, ranging from −22.7 ‰ and −20.1 ‰ (average −21.5 ‰).

4.3. Pollen analysis

A pollen diagram of the DG archaeo-stratigraphic sequence is shown in Fig. 5. A total of 71 pollen types were identified in 145 DG sequence samples. *Pinus*, *Picea*, *Betula*, *Quercus*, and *Carpinus* dominate the tree pollen. The percentage of shrub taxa is relatively low, including *Hippophae* and *Ephedra*. The herbaceous taxa are dominated by *Artemisia*, followed by Amaranthaceae (including Chenopodioideae), Poaceae, *Taraxacum*, *Cirsium*, *Aster*, Ranunculaceae, *Humulus*, aquatic pollen (Cyperaceae, *Typha*, and *Myriophyllum*), and fern spores (*Selaginella*, monolete and trilete spores) were also identified. The algae are dominated by Concentricystes. Based on the stratigraphically constrained cluster analysis (CONISS) of terrestrial pollen percentages, the sequence can be divided into three main pollen assemblage zones, as described below.

Zone I (1215–995 cm): This zone is characterized by high percentages of herbaceous pollen (average of 84 % and the same below), mainly *Artemisia* (38.3 %), Chenopodiodeae (3.9 %), *Cirsium* (16.2 %), *Taraxacum* (11.9 %) and *Aster* (7.9 %). The proportion of tree pollen was relatively high (9.4 %). Conifers included *Pinus* (6.2 %) and *Picea* (1 %), whereas broad-leaved components consisting of *Betula* (1 %) and *Ulmus* (0.6 %), were relatively low. Trilete spores (9.6 %), monolete spores (4.7 %), and aquatic types (5.1 %) were well represented. The total pollen concentration is high in the sequence, averaging 20 grains/g.

Zone II (995–225 cm): This zone is characterized by a pronounced increase in arboreal pollen, mainly *Pinus* (8.5 %), followed by *Picea* (2.1 %), *Betula* (1.7 %), and *Quercus* (1.4 %). Herb pollen content decreases significantly, with *Artemisia* (37.5 %), *Humulus* (12.5 %), Chenopodiodeae (12.4 %), Ranunculaceae (6.2 %), and Poaceae (5.9 %). A sharp decline in the total pollen concentrations to an average of seven grains per gram is observed. Based on changes in pollen assemblages, this zone can be divided into three subzones.

Subzone II-a (995–545 cm): This subzone is characterized by a slow increase in tree pollen. Compared to Zone I, *Cirsium* (1.8 %), *Aster* (1.8 %), and *Taraxacum* (3.8 %) show a significant downward trend, whereas the contents of Chenopodioideae (12.7 %), *Humulus* (11.9 %), Ranunculaceae (7.7 %), and Poaceae (6.4 %) increase significantly.

Subzone II-b (545–465 cm): This subzone is characterized by a sharp increase of tree pollens to the peak of the sequence, representing notable growth of *Pinus* (26.2 %) and *Picea* (17.2 %). The percentage of herbaceous taxa also significantly decreases.

Subzone II-c (465–225 cm): The arboreal pollen content (13.1 %) is consistent with the average value of the entire profile. Notablely, herbaceous pollen (86.9 %) rebounds, mainly *Artemisia* (41.3 %), Chenopodiaceae (13.2 %), and *Humulus* (16.6 %).

Zone III (225–40 cm): This zone is characterized by a high percentage of herbaceous pollen (84.4 %), which is dominated by *Artemisia* (34.5 %) and Chenopodiaceae (10.2 %). Marked increases in *Taraxacum* (15.3 %), *Cirsium* (6.8 %), and *Aster* (3.0 %), and a decrease in *Humulus*

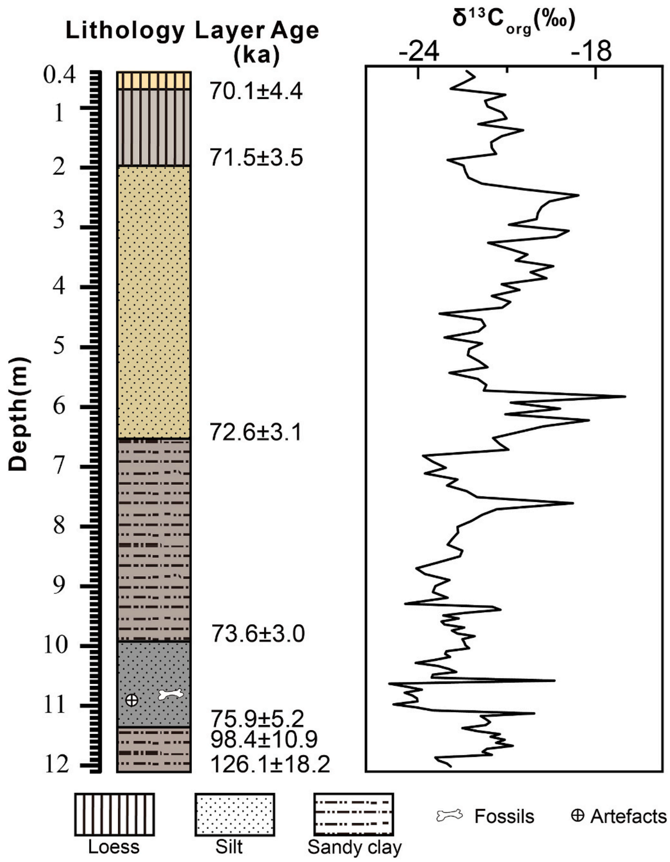

Fig. 4. The $\delta^{13}C_{org}$ values of the Donggou archaeo-stratigraphic sequence.

(2.5 %) are observed. Among the tree pollen types, the content of *Pinus* increases to 11.2 %, whereas the percentages of *Quercus* and *Betula* decrease to 1.4 % and 0.8 % respectively. The total pollen concentration peaks across the entire profile, averaging 116 grains/gram. This zone can be further divided into two subzones: III-a and III-b.

Subzone III-a (225–65 cm), the characteristics of this subzone represent the pollen assemblage of Zone III.

Subzone III-b (65–40 cm), the tree percentage decreases by 13.4 %. Herb pollen types are the dominant taxa; *Artemisia* shows a plummet of 8.8 %, whereas Chenopodiaceae and *Taraxacum* increase significantly to 26.0 % and 29.5 %, respectively.

4.4. Quantitative precipitation

After assessing the pollen dataset and filtering evidently deviated samples, 884 modern pollen samples within a 1000 km radius of the DG site (Fig. 6a) were selected to train the dataset for MAP reconstruction, following the method proposed by Cao et al. (2014). Based on the maximum coefficient of determination (R^2) and minimum root mean square error (RMSEP), the third component of the WAPLS model showed optimal performance for MAP (R^2 = 0.89, RMSE = ± 68.3 mm) (Fig. 6b). The reconstructed MAP values suggest a drier climate in the Nihewan Basin during formation of the DG Site. The MAP ranged from 220 to 561 mm (average 332 mm), indicating drier conditions than those observed today (Fig. 6c). During Layer 6 accumulation, MAP values are relatively high, reaching a peak of 455 mm. During the occupation of the DG hominins, the predicted MAP ranges from 220 to 367 mm, with an average of 290 mm, reflecting more arid conditions. Above 600 cm, MAP showed a decreasing trend, followed by a rapid increase to 561 mm at 500 cm. From 400 cm upward, MAP increases with notable fluctuations.

5. Discussion

5.1. Climate and environmental implications of proxy records

As previously mentioned, the DG archaeo-stratigraphic sequence consists of fluvial floodplain deposits (1215–200 cm) overlain by loess sediments (200–40 cm) (Fig. 1d-e) (Xu et al., 2024). Therefore, we interpret the implications of these environmental proxies based on the two sedimentary units as follows:

Terrestrial plants are divided into C_3 and C_4 types, characterized by stable carbon isotope compositions of −20 to −34 ‰ (average approximately −27 ‰) and −9∼ −19 ‰ (with a mean of −13 ‰) according to their photosynthetic pathways (O'Leary, 1981, 1988; Rao et al., 2013b). C_3 plants are dominated by trees, bushes, and herbaceous plants and prefer cold and humid environments with high CO_2 concentrations. C_4 plants (mainly tropical or semi-tropical herbaceous taxa) tend to grow in hot and arid environments with low atmospheric CO_2 concentrations

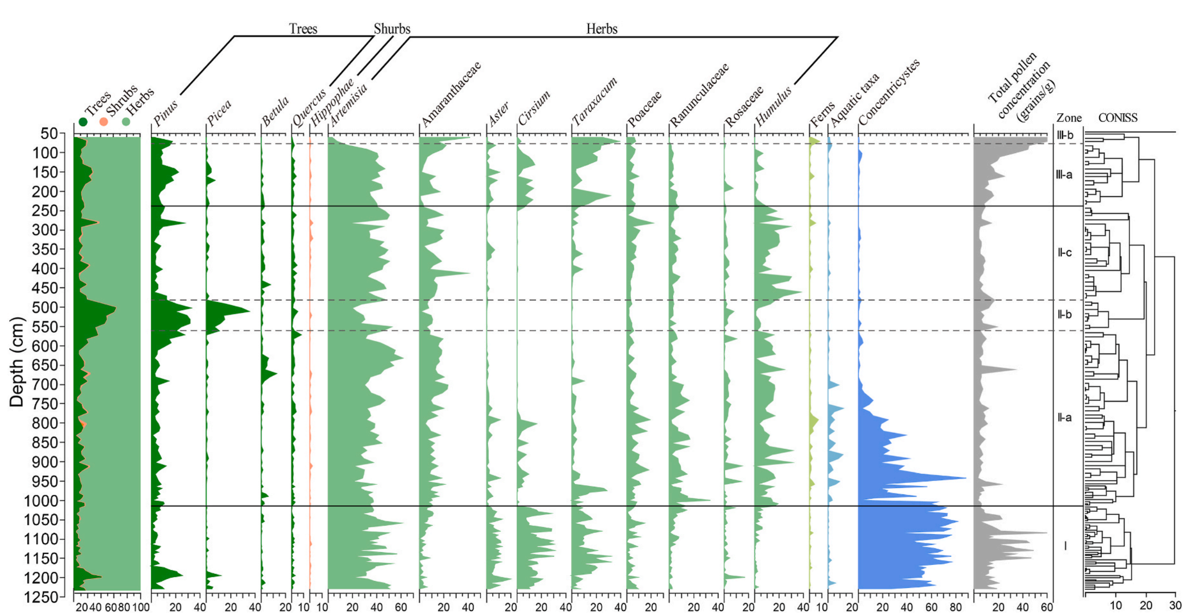

Fig. 5. Pollen percentage diagram and concentration for the Donggou archaeo-stratigraphic sequence. (Only major pollen taxa are shown.)

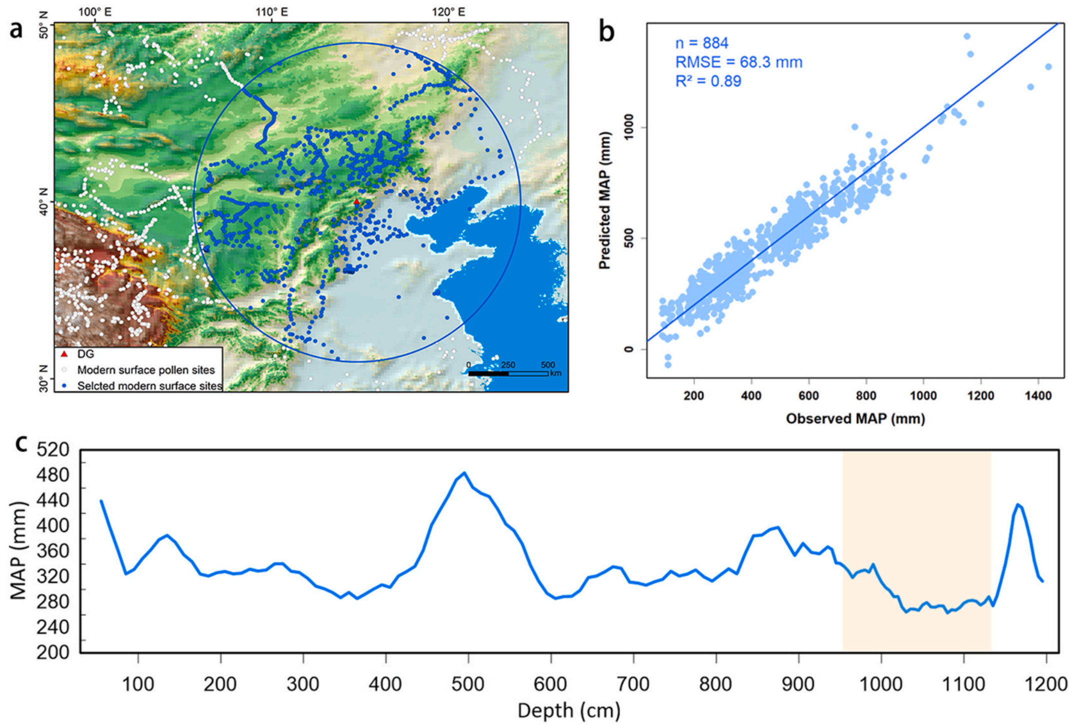

Fig. 6. Quantitative reconstruction of DG site. a. Distribution of the samples in the modern pollen training-set (blue points, n = 884) and the location of the DG site (red triangle). b. Scatter plots of WAPLS predicted MAP versus observed MAP based on the modern pollen training-set. c. Predicated MAP of the pollen-based climate reconstructions for the DG archaeo-stratigraphic sequence (the yellow band represents archaeological layer).

(Gu et al., 2003). The stable isotope composition of total organic carbon has been widely used in loess sequences for paleoclimatic reconstruction to represent the relative abundance of C_3/C_4 plants (Cerling et al., 1989; Liu et al., 2005; Kohn, 2010; Rao et al., 2013b; Ren et al., 2022). Changes in δ^{13}C value are mainly caused by precipitation and broadly correlated with oxygen isotopes (δ^{18}O) of stalagmite from Southern China during the Last Glacial (Liu et al., 2005; Chen et al., 2006b; Rao et al., 2013a). In this study, positive $\delta^{13}C_{org}$ values at the DG site indicate an expansion of C_4 vegetation and suggest drier conditions, while negative values reflect the dominance of C_3 under wetter conditions (Vidic and Montañez, 2004; Rao et al., 2013a). Given the complexity in the sedimentary process in river floodplains, even though the aquatic plants and algae contribute negative values of $\delta^{13}C_{org}$ in fluvial floodplain deposits, they still record regional vegetation and, indirectly, regional climate with similar implications (Erkens et al., 2009; Hoffmann et al., 2009; Gong et al., 2014; Tian et al., 2022).

Serving as a direct proxy of paleovegetation, the pollen assemblage can be used to reconstruct the climatic transition. Based on the depositional process at the DG site (Xu et al., 2024), we infer that the pollen grains in the sequence were mainly transported by surface runoff and wind, representing the surrounding environment. Tree growth requires moisture conditions that reflect regional humidity (Zhang et al., 2022b). Herb pollen types, such as *Artemisia*, Chenopodiaceae, and Poaceae are typical steppe taxa, the percentages of which represent steppe expansion or contraction. Aquatic pollen types, such as Cyperaceae and algae (Concentricystes), indicate the presence of wetlands or floodplain environments adjacent to the site. The total pollen concentration indicates the vegetation cover around the site (Chen et al., 2006a).

5.2. Climate, environmental variations, and hominin occupation during the DG site formation

Due to the sedimentary hiatus between Layer 6 and Layer 5, as mentioned earlier, we focus on the environmental records above Layer 5 (1135–40 cm; 75.9–70.5 ka). Linear interpolation was applied to estimate the age of each sample for environmental reconstruction (Blaauw and Christen, 2011), thereby providing a chronological framework for interpreting the climatic and environmental proxies. Based on $\delta^{13}C_{org}$, pollen assemblages, and a quantitative reconstruction of MAP from the DG sequence, we reconstructed paleoclimate changes during the MIS 5–4 transition in the Nihewan Basin. The history of climatic changes is correlated with the δ^{18}O records from stalagmite (Cheng et al., 2016) and the Greenland ice core (the North Greenland Ice Core Project, NGRIP) (Seierstad et al., 2014). A coherent interpretation of these correlations is presented in Fig. 7. Five distinct stages were identified, encompassing the Heinrich events (H7) and Dansgaard-Oeschger events (DO19 and DO20), which described in detail below.

Stage 1 (75.6ka –74 ka): As the main phase of hominin occupation at the DG site, this period is characterized by the driest climate in the whole sequence. This stage corresponded to the upper part of pollen Zone I and the lower part of pollen Zone II when arboreal pollen percentages were relatively low and herbaceous taxa were dominant, particularly *Artemisia* and Chenopodiaceae, indicating a temperate, dry climate. However, the total pollen concentration, influenced by abundant algae, was relatively high, reflecting a moist environment adjacent to the river. The overall negative shift in $\delta^{13}C_{org}$ values during this period may reflect combined contributions from aquatic plants and C_3 terrestrial vegetation. The quantitative reconstruction of precipitation (average MAP = 290 mm) yielded the lowest value in the sequence, which correlated with other proxies and indicate an open steppe environment under cold, arid conditions. In this context, DG hominins occupied the floodplain margin as inhabitants of a resource-limited environment.

Stage 2 (74ka –73.1ka): This stage was characterized by increasing regional humidity, accompanied by an increase in arboreal pollen and MAP. The negative shift in $\delta^{13}C_{org}$ values and the peaks in MAP correspond with negative values observed in the δ^{18}O records of stalagmites from South China, indicating an intensification of the East Asian Summer Monsoon accompanied by increased rainfall in the monsoon-

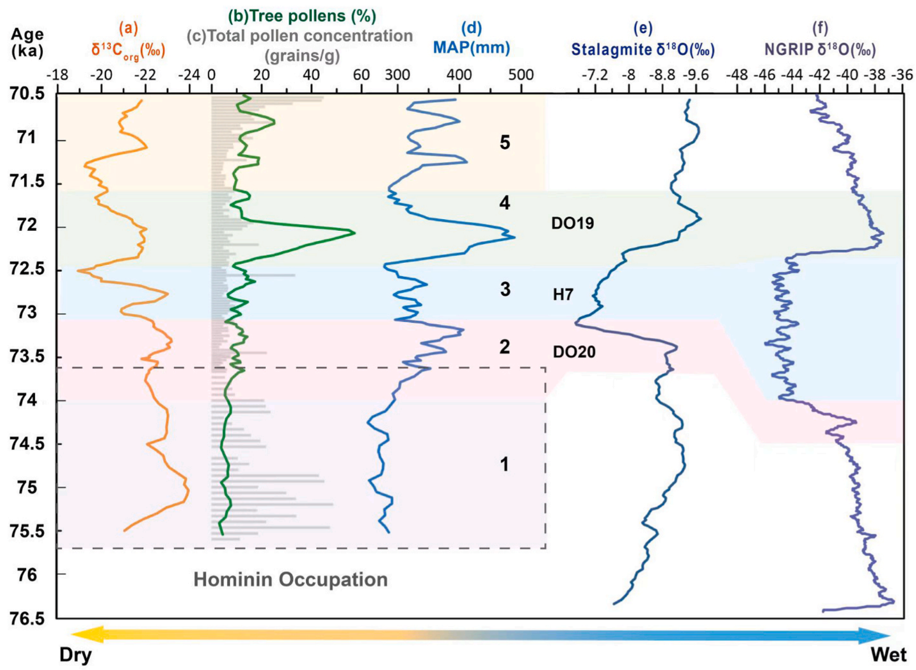

Fig. 7. Comparison of paleoenvironmental proxy records from Donggou site, Chinese speleothem oxygen isotope records (Cheng et al., 2016) and NGRIP oxygen isotope records (Seierstad et al., 2014). (a) $\delta^{13}C_{org}$ (‰); (b) Tree pollen percentages (%); (c) Bar chart of total pollen concentration (grains/g); (d) Reconstructed MAP (mm); (e) $\delta^{18}O$ records of stalagmite South China (‰); (f) $\delta^{18}O$ records of NGRIP (‰). (All curves were smoothed using a moving average).

dominated eastern China (Cheng et al., 2016). The increase in $\delta^{18}O$ reflects rising temperatures in the Northern Hemisphere (Seierstad et al., 2014). Combined with multiple global and regional climate records (Seierstad et al., 2014; Yang and Ding, 2014), we inferred that this phase in the Nihewan Basin may be consistent with DO 20 (Fig. 7). Compared to the previous stage, the climate became milder and wetter, likely sustaining the continuous occupation of the DG hominins.

Stage 3 (73.1ka –72.5ka): Along with the intensive aridity of the region, this site was abandoned by hominins. Tree pollen was dominated by *Pinus* and *Picea*, with a decrease in broadleaf forests in the nearby mountains. Simultaneously, xerophytic shrubs and herbs began to develop around the site, indicating the expansion of the steppe. A positive fluctuation in $\delta^{13}C_{org}$ values corresponds with this pattern. The total vegetation cover and MAP decreased to their lowest values over the entire sequence. These environmental indicators are associated with high $\delta^{18}O$ values in stalagmite records and low $\delta^{18}O$ values in ice cores, suggesting cool–dry climate conditions and ecological degradation of the steppe environment during Heinrich Event (H7), in the Nihewan Basin.

Stage 4 (72.5ka –71.6ka): This stage is characterized by rapid humidity recovery. The percentage of tree pollen increased sharply at its peak, indicating an expanded forest. *Artemisia* was dominant in the herbs, indicating increased humidity. With tree expansion, $\delta^{13}C_{org}$ values showed a negative trend, and MAP reached the peak of 590 mm. This pattern aligns with the negative excursion in stalagmite $\delta^{18}O$ and the increased $\delta^{18}O$ values in ice cores (Fig. 7), suggesting a mild, humid climate condition and temporary forest expansion during an interstadial corresponding to DO 19.

Stage 5 (71.6ka −70.6ka): This period was more moderate and drier than the preceding period. Patches of broad-leaved deciduous woodlands have developed in the surrounding mountains. Herbaceous plants were mainly Asteraceae (*Taraxacum*, *Cirsium*, *Aster*, and *Artemisia*) and Chenopodiaceae. The low abundance of mesophytic and moisture-demanding plants indicated a mild and dry regional climate. Increasing $\delta^{13}C_{org}$ values indicate the expansion of drought-tolerant C4 plants. MAP showed a marked decrease compared to the previous stage, followed by stable fluctuations and a gradual increase after 70.8 ka. Together, these proxies indicated an increasingly arid regional steppe environment in the Nihewan Basin with the advent of MIS 4.

Paleoenvironmental reconstruction of the DG site suggests that the overall regional climate of the MIS 5–4 transition was drier and colder than it is today. First, Donggou hominins adapted to cold and arid steppe environments by choosing natural resource-rich floodplains as their habitats. The climatic recovery of DO20 sustained continuous hominin occupation. Thus, the ecological degradation at H7 may have driven the hominin population away from the site.

In summary, hominins exhibit excellent resilience in unstable environments. However, interstadials in the MIS 5–4 transition provided optimal conditions for hominins in the Nihewan Basin. Intermittent aridity at the end of MIS 5a was even more severe than the initial MIS 4 conditions in the basin, whereas the adaptive capabilities of hominins when facing increasing climatic severity and changing landscapes suggest its potential to survive in the coming MIS 4.

5.3. *Implications for hominin behavioral adaptations in the Nihewan Basin during the MIS 5–4 transition*

Understanding the evolution of subsistence strategies during this period of environmental change is of prime interest for understanding how regional climate fluctuations drive human evolution and behavioral adaptations (Potts, 2013; deMenocal and Stringer, 2016; Timmermann and Friedrich, 2016; Wang H et al., 2024; Zan et al., 2024). In this context, the results of our study provide valuable clues to link hominin adaptive strategies with ecological and landscape shifts and to explore potential externally driven mechanisms behind hominin behavioral evolution in the Nihewan Basin during the MIS 5–4 transition, a period marked by increasing instability in regional environments (Wang et al., 2001, 2008b, 2021; Xiong et al., 2002; Guan et al., 2010).

The DG site is located in the Yuxian sub-basin, which has been generally recognized as a part of the Nihewan paleolake since the Late Pliocene (Xia and Liu, 1984; Deng et al., 2008; Ao et al., 2013; Tang et al., 2020), preserving the deposition of Late Pliocene to Middle Pleistocene fluvio-lacustrine sediments (Cai et al., 2013; Yuan et al., 2011). Current evidence indicates that the Nihewan paleolake gradually retreated during the Middle Pleistocene, resulting in the development of the Sanggan River (in the Yangyuan sub-basin) between approximately 270 and 86 ka ago (Guo et al., 2016). It developed with the formation of its tributaries, including the Huliu River in the Yuxian sub-basin (Zhou et al., 1991; Xie et al., 2006; Yuan et al., 2011). The transformation from lacustrine to fluvial environments created new landscapes for hominins. With the widespread development of river terraces in the Yuxian sub-basin, the availability of fresh water, animal resources, and fluvial gravel (as lithic raw materials), had created attractive habitats for hominin adaptations to regional landforms and climate fluctuations since the last interglacial and glacial periods.

Our study established a high-resolution chronological framework (75.9–70.5 ka) in the Nihewan Basin using OSL dating, coupled with paleoclimatic records, which corresponds to critical climate events during the MIS 5–4 transition. The results indicate that DG hominins occupied this site from 75.9 to 73.6 ka (Fig. 3). Combining climate reconstruction with fossil assemblages, including *Bovidae*, *Cervus*, *Equus*, *Meles*, and *Gazella*, the DG hominins experienced an expanding arid steppe environment at the end of MIS 5. Faced with the intensified aridity of this region, DG hominins have developed diverse strategies to adapt to the cold, arid steppe environments. With the landscape shift from the Nihewan paleolake to the development of the DG River system (a tributary of the Ding'an River), DG hominins chose river floodplains as habitats under increasingly arid regional conditions. They made full use of low-density and patchy resources. In addition to collecting fluvial gravel from river channels for flaking, DG hominins showed novel patterns that procured high-quality chalcedony, opal, and agate (Fig. 2h–m) to create elaborate tools rather than for intensive use, demonstrating a novel approach to a wider resource procurement strategy and the efficient utilization of high-quality materials (Zhou et al., 2024). Second, alternative freehand and bipolar flaking techniques (Fig. 2a–d, f, g, i) demonstrates the technological flexibility of DG knappers at the site (Zhou et al., 2024). In addition to a high proportion of retouched tools (5.4 %), the DG lithic assemblage showed a diversity of tool types and a certain degree of standardization, as scrapers, denticulates and pointed tools presented distinct features (Fig. 2e, h, j–m) and refined retouching of small-sized tools highlighting the significant manual precision of DG hominins. Such refined tools may be used to acquire and consume animal tissues (Conard and Prindiville, 2000; Stiner, 2013), as demonstrated by the current research on DG fossils (He, 2025). Complementary taphonomic analyses revealed the systematic exploitation of animal resources, including defleshing, marrow extraction, and skinning (Fig. 2n and o and Fig. 8), as evidenced by the cutmarks in the ungulate metapodial (Fig. 2o) with dissection at the epiphyseal junctions preserving fur integrity, suggesting the potential use of animal skin and fur (Charles, 1997) (Fig. 8). At the DG site, burnt bones (Fig. 2p) and stones demonstrated that hominins adopted a fire-use strategy under cold conditions. These multifaceted behavioral adaptations may have significantly enhanced DG hominins' adaptability to hostile and variable environments during the MIS 5–4 transition.

Fluctuations in climate and environment (see Fig. 8a for the corresponding paleoclimatic records of NGRIP) play a pivotal role in driving hominin demographic expansions and behavioral adaptations. In the Nihewan Basin, the environmental sequence of the Youfang site, dated to MIS 5d–b, indicates frequent landscape transitions from desert steppe to forest (Li et al., 2024). Stratigraphic records at Xinmiaozhuang Locality 1 evidence dramatic climatic fluctuations during the MIS 5–4 transition (Wang et al., 2021). Meanwhile, several advanced technological strategies, including new technological elements such as discoidal cores, elongated flakes, and finely retouched tools (Mousterian-like tools), were recovered at 100–70 ka (Yang et al., 2020; Wang et al., 2021; Ren et al., 2025). At the terminal MIS 5, abundant discoidal cores and elongated flakes were observed at the Banjingzi site (86±4ka) (Guo et al., 2016; Ren et al., 2025), and primary analyses of animal remains showed adequate exploitation of horses (Wang X et al., 2024). The lithic assemblage at Xinmiaozhuang Locality 1 (75ka −63 ka), characterized

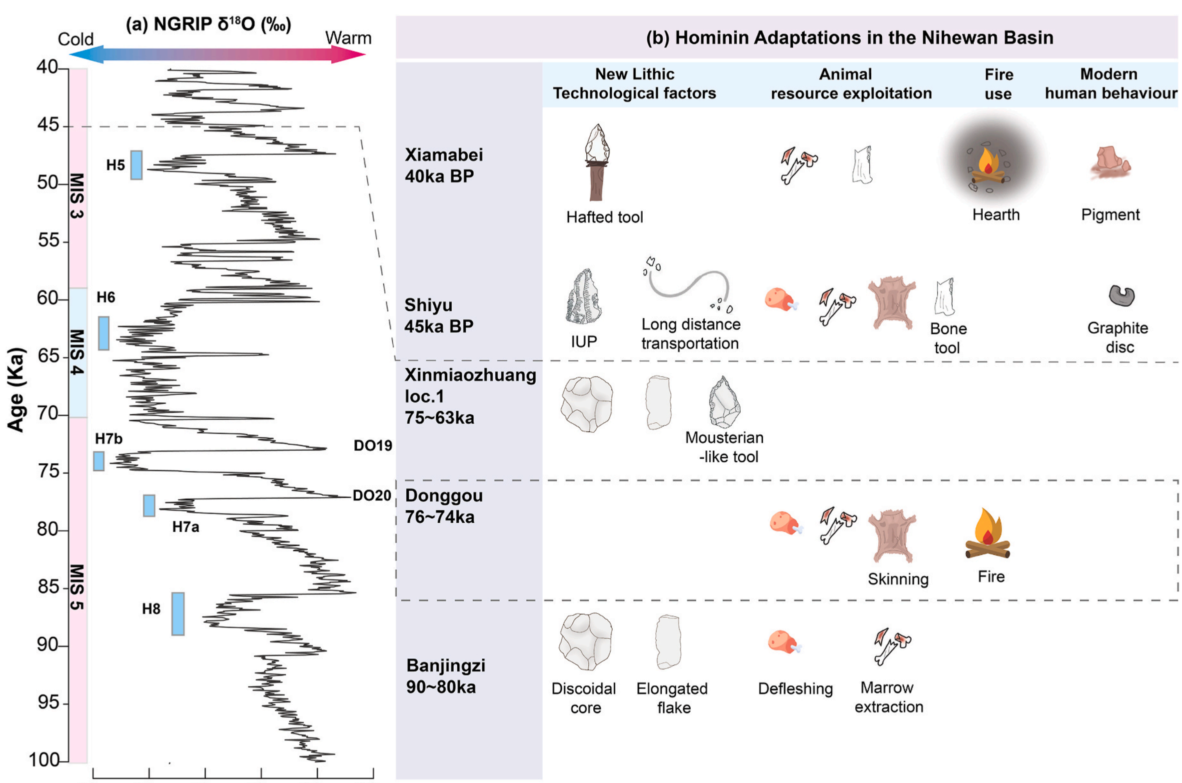

Fig. 8. Oxygen isotope records of NGRIP and hominin adaptations in the Nihewan Basin (100∼40ka). (a) $\delta^{18}O$ records of NGRIP from 100 to 40 ka (‰) (only partial events were marked) (Seierstad et al., 2014); (b) Hominin adaptations in the Nihewan Basin.

by discoidal cores, Mousterian-affiliated prepared cores, and specialized toolkits (Fig. 8), exemplifies the advanced developmental phase of North China's small-tool industry (Wang et al., 2021).

Filling the behavioral trajectory sequence composed of these sites, the occupation of DG hominins during the advent of MIS 4, despite the lack of new technological elements, represents the aforementioned adaptive strategy (including specialized resource exploitation and fire use) (Fig. 8) and represents a diversified behavioral response to an increasingly challenging environment. Much evidence suggests that the behavioral diversification that occurred during the MIS 5–4 transition may indicate the indigenous behavioral evolution of archaic hominins before the arrival of modern humans in the Nihewan Basin. Following MIS 4, hominin adaptive strategies underwent abrupt and substantial shifts (Fig. 8), marked by technological innovations (such as hafted tools) and the emergence of modern human behavior (graphite discs at Shiyu and pigment use at Xiamabei) (Wang et al., 2022; Yang et al., 2024). These changes are recognized as evidence of the expansion of *H. sapiens*, characterized by highly complex and innovative behavioral traits. Altogether, in the context of the Nihewan Basin, behavioral diversification and technological flexibility likely reflect adaptive strategies adopted by local hominins in response to fluctuating environments during the early Late Pleistocene. These sites, characterized by subtle variations such as new technological elements and diverse resource-use strategies, indicate consistent and flexible adaptive behaviors rather than abrupt technological innovation. The observed behavioral variability and increasing adaptive capacity suggest that technological flexibility, together with enhanced cognitive capabilities, resulted from long-term adjustments of local hominins in response to fluctuating environmental conditions since the MIS 5–4 transition. This adaptive trajectory was later accelerated by the arrival of modern humans approximately 45 ka later.

6. Conclusions

The transition from MIS 5 to 4 marked a sudden shift in global climate change and created new environmental conditions for human evolution, dispersal, and adaptation. In this study, environmental proxies of pollen and stable carbon isotope ($\delta^{13}C_{org}$) analysis coupled with reliable OSL dating ages were used to interpret the temporally based environmental records represented in the DG archaeo-stratigraphic sequence from the Nihewan Basin and link the hominin behavioral adaptations to the climate fluctuation, and the main conclusions are as follows:

1) High-resolution MET-pIRIR stimulated luminescence dating method on multi-grain single-aliquot and single-grain potassium feldspars indicates that the DG site formed during the period of 70.1 ± 4.4 ka and 126.1 ± 18.2 ka, falling within the MIS 5 and transition to MIS 4. The archaeological layer is bracketed between 75.9 ± 5.2 ka and 73.6 ± 3.0 ka, indicating hominin occupation around 76 to 74 ka and corresponding to the late phase of MIS 5a in the Nihewan Basin.
2) The $\delta^{13}C_{org}$ values, pollen spectra, and quantitative reconstruction of precipitation from the DG archaeo-stratigraphic sequence provided a paleoenvironmental record of the transition from MIS 5 to MIS 4, identifying signals of millennial-scale climatic events including DO20, H7, and DO19 events. The regional climate shifted from temperate humid forests to sparse forest grasslands and desert steppes during site formation. The DG hominins persisted in the initial arid phase. They continued to occupy the river floodplain landscape during the mild and moist DO20 events of late MIS 5a, before the climate deterioration of MIS 4.
3) The DG hominins occupying the northern high latitudes of the Nihewan Basin adapted successfully to challenging local environments and developed flexible and innovative behavioral strategies. Such strategies include the sufficient exploitation of high-quality lithic raw material, the use of freehand and bipolar flaking techniques, an increased number of retouched tools, systematic and efficient exploitation of ungulates, and even the use of fire. Such flexible adaptations, together with regional archaeological evidence from the Nihewan Basin spanning the last interglacial and glacial stages, led us to hypothesize that hominin behavioral diversification occurred in response to the fluctuating environment before the emergence of *H. sapiens* in the Nihewan Basin.

Overall, our findings suggest that the increased technological variability associated with the MIS 5–4 transition may have played a critical role in shaping the affordances available to DG hominins and in contributing to the emergence of novel behavioral diversification responses to regional climatic challenges.

Funding

This research was supported by the National Social Science Foundation of China (21BKG034).

Declaration of competing interest

The authors declare that they have no known competing financial interests or personal relationships that could have appeared to influence the work reported in this paper.

Acknowledgements

We would like to thank Dr. Junchi Liu from the Institute of Vertebrate Paleontology and Paleoanthropology, Chinese Academy of Sciences, for his kind guidance and support during the experiments. We are also grateful to Drs. Xin Ding, Dongdong Ma, and Mr. Guangyi Bai from Institute of Vertebrate Paleontology and Paleoanthropology (CAS) for their helpful discussions. Thanks Mr. Shihang Zhou from Jilin University for providing relevant images. Mr. Xiangdong He and Ms. Bingrou Huang from Hebei Normal University are thanked for valuable insights into taphonomy and work on OSL dating, respectively. Mr. Feng Xue (also from Hebei Normal University) provided assistance with fieldwork. We further thank the officials and cultural heritage staff of Hebei Province, as well as the local authorities in Yuxian County, for facilitating field investigations. We take full responsibility for any remaining errors.

Appendix B. Supplementary data

Supplementary data to this article can be found online at https://doi.org/10.1016/j.quascirev.2025.109714.

Data availability

The original data presented in the study are available in the main text, further inquiries can be directed to the corresponding author upon reasonable request.

References

Ao, H., Dekkers, M.J., An, Z., Xiao, G., Li, Y., Zhao, H., Qiang, X., Chang, H., Chang, Q., Wu, D., 2013. Magnetostratigraphic evidence of a mid-Pliocene onset of the Nihewan formation – implications for early fauna and hominid occupation in the Nihewan Basin, north China. Quat. Sci. Rev. 59, 30–42. https://doi.org/10.1016/j.quascirev.2012.10.025.

Ao, H., Ruan, J., Martinón-Torres, M., Krapp, M., Liebrand, D., Dekkers, M.J., Caley, T., Jonell, T.N., Zhu, Z., Huang, C., Li, X.X., Zhang, Z., Sun, Q., Yang, P., Jiang, J., Li, X. Z., Xie, X., Song, Y., Qiang, X., Zhang, P., An, Z., 2024. Concurrent Asian monsoon strengthening and early modern human dispersal to east Asia during the last interglacial. Proc. Natl. Acad. Sci. USA 121, e2308994121. https://doi.org/10.1073/pnas.2308994121.

Bae, C.J., 2017. Late Pleistocene human evolution in eastern Asia: behavioral perspectives. Curr. Anthropol. 58, S514–S526. https://doi.org/10.1086/694078.

Bae, C.J., 2024a. The Paleoanthropology of Eastern Asia. University of Hawaii Press, Honolulu. ISBN: 978-0-8248-9-7659.
Bae, C.J., 2024b. Modern humans in northeast Asia. Nat. Ecol. Evol. 8, 368–369. https://doi.org/10.1038/s41559-023-02316-1.
Bae, C.J., Douka, K., Petraglia, M.D., 2017. On the origin of modern humans: asian perspectives. Science 358, eaai9067. https://doi.org/10.1126/science.aai9067.
Bae, C.J., Li, F., Cheng, L., Wang, W., Hong, H., 2018. Hominin distribution and density patterns in Pleistocene China: climatic influences. Palaeogeogr. Palaeoclimatol. Palaeoecol., Cenozoic Climate Change in Eastern Asia - PART II 512, 118–131. https://doi.org/10.1016/j.palaeo.2018.03.015.
Bae, C.J., Wang, W., Zhao, J., Huang, S., Tian, F., Shen, G., 2014. Modern human teeth from late Pleistocene Luna cave (Guangxi, China). Quat. Int., Multidisciplinary Perspectives on the Gigantopithecus Fauna and Quaternary Biostratigraphy in East Asia 354, 169–183. https://doi.org/10.1016/j.quaint.2014.06.051.
Barbour, G.B., 1924. Preliminary observations in the Kalgan area. Bull. Geol. Surv. Can. 3, 153–168. https://doi.org/10.1111/j.1755-6724.1924.mp3002009.x.
Tracking environmental change using lake sediments: data handling and numerical techniques. In: Birks, H.J.B., Lotter, A.F., Juggins, S., Smol, J.P. (Eds.), 2012. Developments in Paleoenvironmental Research. Springer, Netherlands, Dordrecht. https://doi.org/10.1007/978-94-007-2745-8.
Blaauw, M., Christen, J.A., 2011. Flexible paleoclimate age-depth models using an autoregressive gamma process. Bayesian Anal 6 (3), 457–474. https://doi.org/10.1214/11-BA618.
Blunier, T., Brook, E.J., 2001. Timing of millennial-scale climate change in Antarctica and Greenland during the last glacial period. Science 291 (5501), 109–112. https://doi.org/10.1126/science.291.5501.109.
Cai, B.Q., Zheng, S.H., Liddicoat, J.C., Li, Q., 2013. Review of the litho-, bio-, and chronostratigraphy in the Nihewan Nasin, Hebei, China. In: Wang, X.M., Flynn, L.J., Fortelius, M. (Eds.), Fossils of Asia: Neogene Biostratigraphy and Chronology. Columbia University Press, New York, pp. 218–242.
Cao, X., Herzschuh, U., Telford, R.J., Ni, J., 2014. A modern pollen–climate dataset from China and Mongolia: assessing its potential for climate reconstruction. Rev. Palaeobot. Palynol. 211, 87–96. https://doi.org/10.1016/j.revpalbo.2014.08.007.
Cerling, T.E., Quade, J., Wang, Y., Bowman, J.R., 1989. Carbon isotopes in soils and palaeosols as ecology and palaeoecology indicators. Nature 341, 138–139. https://doi.org/10.1038/341138a0.
Charles, R., 1997. The exploitation of carnivores and other fur-bearing mammals during the north-western European late and upper Paleolithic and Mesolithic. Oxf. J. Archaeol. 16, 253–277. https://doi.org/10.1111/1468-0092.00040.
Chen, F., Cheng, B., Zhao, Y., Zhu, Y., Madsen, D.B., 2006a. Holocene environmental change inferred from a high-resolution pollen record, Lake Zhuyeze, arid China. Holocene 16, 675–684. https://doi.org/10.1191/0959683606hl951rp.
Chen, F., Rao, Z., Jiawu, Z., Ming, J., Jianying, M., 2006b. Variations of organic carbon isotopic composition and its environmental significance during the last glacial on western Chinese Loess Plateau. Chin. Sci. Bull. 51, 1593–1602. https://doi.org/10.1007/s11434-006-2003-6.
Cheng, H., Edwards, R.L., Sinha, A., Spötl, C., Yi, L., Chen, S., Kelly, M., Kathayat, G., Wang, X., Li, X., Kong, X., Wang, Y., Ning, Y., Zhang, H., 2016. The Asian monsoon over the past 640,000 years and ice age terminations. Nature 534, 640–646. https://doi.org/10.1038/nature18591.
Conard, N.J., Prindiville, T.J., 2000. Middle Palaeolithic hunting economies in the Rhineland. Int. J. Osteoarchaeol. 10, 286–309. https://doi.org/10.1002/1099-1212(200009/10)10:5<286::AID-OA557>3.0.CO;2-8.
deMenocal, P.B., Stringer, C., 2016. Climate and the peopling of the world. Nature 538, 49–50. https://doi.org/10.1038/nature19471.
Deng, C., Hao, Q., Guo, Z., Zhu, R., 2019. Quaternary integrative stratigraphy and timescale of China. Sci. China Earth Sci. 62, 324–348. https://doi.org/10.1007/s11430-017-9195-4.
Deng, C.L., Zhu, R.X., Zhang, R., Ao, H., Pan, Y.X., 2008. Timing of the Nihewan formation and faunas. Quat. Res. 69, 77–90. https://doi.org/10.1016/j.yqres.2007.10.006.
Erkens, G., Dambeck, R., Volleberg, K.P., Bouman, M.T.I.J., Bos, J.A.A., Cohen, K.M., Wallinga, J., Hoek, W.Z., 2009. Fluvial terrace formation in the northern upper rhine graben during the last 20000 years as a result of allogenic controls and autogenic evolution. Geomorphology 103, 476–495. https://doi.org/10.1016/j.geomorph.2008.07.021.
Faegri, K., Iversen, J., Kaland, P.E., Krzywinski, K., 2000. Textbook of Pollen Analysis. Blackburn Press.
Fick, S.E., Hijmans, R.J., 2017. WorldClim 2: new 1-km spatial resolution climate surfaces for global land areas. Int. J. Climatol. 37, 4302–4315. https://doi.org/10.1002/joc.5086.
Fu, Q., Meyer, M., Gao, X., Stenzel, U., Burbano, H.A., Kelso, J., Pääbo, S., 2013. DNA analysis of an early modern human from Tianyuan Cave, China. Proc. Natl. Acad. Sci. USA 110, 2223–2227. https://doi.org/10.1073/pnas.1221359110.
Gong, Z., Li, S.-H., Li, B., 2014. The evolution of a terrace sequence along the manas river in the northern foreland basin of tian Shan, China, as inferred from optical dating. Geomorphology 213, 201–212. https://doi.org/10.1016/j.geomorph.2014.01.009.
Grimm, E.C., 2019. Tilia Version 2.6.1.
Grove, M., 2014. Evolution and dispersal under climatic instability: a simple evolutionary algorithm. Adapt. Behav. 22, 235–254. https://doi.org/10.1177/1059712314533573.
Gu, Z., Liu, Q., Xu, B., Han, J., Yang, S., Ding, Z., Liu, T., 2003. Climate as the dominant control on C3 and C4 plant abundance in the Loess plateau: organic carbon isotope evidence from the last glacial-interglacial loess-soil sequences. Chin. Sci. Bull. 48, 1271–1276. https://doi.org/10.1007/BF03183950.
Guan, Q.Y., Pan, B.T., Li, N., Li, Q., Zhang, J.D., Gao, H.S., Liu, J., 2010. A warming interval during the MIS 5a/4 transition in two high-resolution loess sections from China. J. Asian Earth Sci. 38, 255–261. https://doi.org/10.1016/j.jseaes.2010.02.004.
Guo, Y.J., Li, B., Zhang, J.F., Yuan, B.Y., Xie, F., Roberts, R.G., 2016. Luminescence ages for three 'Middle Palaeolithic' sites in the Nihewan Basin, northern China, and their archaeological and palaeoenvironmental implications. Quat. Res. 85 (3), 456–470. https://doi.org/10.1016/j.yqres.2016.03.002.
He, X.D., 2025. Preliminary Study on Animal Fossils Unearthed from Donggou Site in Yuxian Basin (master's Thesis). Hebei Normal University, Shijiazhuang.
Hemming, S.R., 2004. Heinrich events: massive late Pleistocene detritus layers of the north Atlantic and their global climate imprint. Rev. Geophys. 42. https://doi.org/10.1029/2003RG000128, 2003RG000128.
Hoffmann, T., Glatzel, S., Dikau, R., 2009. A carbon storage perspective on alluvial sediment storage in the Rhine catchment. Geomorphology 108, 127–137. https://doi.org/10.1016/j.geomorph.2007.11.015.
Huang, B., Niu, D., Pei, S., Guo, Y., 2025. Luminescence age of the Donggou site in the Yuxian Basin. Acta Anthropol. Sin. 1–16. https://doi.org/10.16359/j.1000-3193/AAS.2025.0050.
Juggins, S., 2009. Rioja: analysis of Quaternary science data. https://doi.org/10.32614/CRAN.package.rioja.
Keates, S.G., 2010. Evidence for the earliest Pleistocene hominid activity in the Nihewan basin of northern China. Quat. Int., Oldest Human Expansions in Eurasia: Favouring and Limiting Factors 223–224, 408–417. https://doi.org/10.1016/j.quaint.2010.01.017.
Kohn, M.J., 2010. Carbon isotope compositions of terrestrial C3 plants as indicators of (paleo)ecology and (paleo)climate. Proc. Natl. Acad. Sci. 107, 19691–19695. https://doi.org/10.1073/pnas.1004933107.
Kuhn, S.L., 2019. Initial upper Paleolithic: a (near) global problem and a global opportunity. Archaeol. Res. Asia 17, 2–8. https://doi.org/10.1016/j.ara.2018.10.002.
Li, B., Du, T.Y., Mei, H.J., Wu, M.J., Ma, Q.H., Guo, Y.J., Yi, S.W., Li, Y.C., 2024. The relationship between human activities, climate and vegetation in Youfang site during MIS 5, Nihewan Basin. Quat. Sci. 44 (5), 1322–1337. https://doi.org/10.11928/j.issn.1001-7410.2024.05.19.
Li, F., 2024. Research progress and prospects on northern dispersal routes of early modern humans into east Asia. Acta Anthropol. Sin. 43, 951. https://doi.org/10.16359/j.1000-3193/AAS.2024.0087.
Li, F., Bae, C.J., Ramsey, C.B., Chen, F., Gao, X., 2018. Re-dating Zhoukoudian Upper Cave, northern China and its regional significance. J. Hum. Evol. 121, 170–177. https://doi.org/10.1016/j.jhevol.2018.02.011.
Li, F., Kuhn, S.L., Bar-Yosef, O., Chen, F., Peng, F., Gao, X., 2019a. History, chronology and techno-typology of the upper paleolithic sequence in the Shuidonggou area, northern China. J. World Prehist. 32, 111–141. https://doi.org/10.1007/s10963-019-09129-w.
Li, F., Vanwezer, N., Boivin, N., Gao, X., Ott, F., Petraglia, M., Roberts, P., 2019b. Heading north: late Pleistocene environments and human dispersals in central and eastern Asia. PLoS One 14, e0216433. https://doi.org/10.1371/journal.pone.0216433.
Li, F., Petraglia, M., Roberts, P., Gao, X., 2020. The northern dispersal of early modern humans in eastern Eurasia. Sci. Bull. 65, 1699–1701. https://doi.org/10.1016/j.scib.2020.06.026.
Li, X., Pei, S., Jia, Z., Guan, Y., Niu, D., Ao, H., 2016. Paleoenvironmental conditions at Madigou (MDG), a newly discovered early Paleolithic site in the Nihewan Basin, North China. Quat. Int. 400, 100–110. https://doi.org/10.1016/j.quaint.2015.07.071.
Liu, W., Huang, Y., An, Z., Clemens, S.C., Li, L., Prell, W.L., Ning, Y., 2005. Summer monsoon intensity controls C4/C3 plant abundance during the last 35 ka in the Chinese Loess Plateau: carbon isotope evidence from bulk organic matter and individual leaf waxes. Palaeogeogr. Palaeoclimatol. Palaeoecol. 220, 243–254. https://doi.org/10.1016/j.palaeo.2005.01.001.
Liu, W., Jin, C.Z., Zhang, Y.Q., Cai, Y.J., Xing, S., Wu, X.J., Cheng, H., Edwards, R.L., Pan, W.S., Qin, D.G., An, Z.S., Trinkaus, E., Wu, X.Z., 2010a. Human remains from Zhirendong, south China, and modern human emergence in East Asia. Proc. Natl. Acad. Sci. USA 107, 19201–19206. https://doi.org/10.1073/pnas.1014386107.
Liu, W., Wu, X.Z., Pei, S., Wu, X.J., Norton, C.J., 2010b. Huanglong Cave: a late pleistocene human fossil site in Hubei Province, China. Quat. Int., hominin morphological and behavioral variation in Eastern Asia and Australasia. Current Perspectives 211, 29–41. https://doi.org/10.1016/j.quaint.2009.06.017.
Liu, W., Martinón-Torres, M., Cai, Y., Xing, S., Tong, H., Pei, S., Sier, M.J., Wu, Xiaohong, Edwards, R.L., Cheng, H., Li, Y., Yang, X., de Castro, J.M.B., Wu, Xiujie, 2015. The earliest unequivocally modern humans in southern China. Nature 526, 696–699. https://doi.org/10.1038/nature15696.
Lu, J., Xu, Q., Liu, Y., Hu, Y., Li, M., Zhang, S., 2018. Holocene environmental changes and human activity at the Jijitan site in the Nihewan Basin, China. Holocene 28 (6), 095968361876154. https://doi.org/10.1177/0959683618761544.

O'Leary, M.H., 1988. Carbon isotopes in photosynthesis: fractionation techniques may reveal new aspects of carbon dynamics in plants. Bioscience 38, 328–336. https://doi.org/10.2307/1310735.

O'Leary, M.H., 1981. Carbon isotope fractionation in plants. Phytochemistry 20, 553–567. https://doi.org/10.1016/0031-9422(81)85134-5.

Pei, S., Deng, C., De La Torre, I., Jia, Z., Ma, D., Li, X., Wang, X., 2019. Magnetostratigraphic and archaeological records at the Early Pleistocene site complex of Madigou (Nihewan Basin): implications for human adaptations in North China. Palaeogeogr. Palaeoclimatol. Palaeoecol. 530, 176–189. https://doi.org/10.1016/j.palaeo.2019.05.014.

Pei, S.W., Wang, F.G., Niu, D.W., 2024. A general review on the discovery and research progress of hominins in the Nihewan Basin since the 21st century. Acta Anthropol. Sin. 43, 913–933. https://doi.org/10.16359/j.1000-3193/AAS.2024.0086.

Potts, R., 2013. Hominin evolution in settings of strong environmental variability. Quat. Sci. Rev. 73, 1–13. https://doi.org/10.1016/j.quascirev.2013.04.003.

Potts, R., 2012. Evolution and environmental change in early human Prehistory. Annu. Rev. Anthropol. 41, 151–167. https://doi.org/10.1146/annurev-anthro-092611-145754.

Potts, R., Behrensmeyer, A.K., Faith, J.T., Tryon, C.A., Brooks, A.S., Yellen, J.E., Deino, A. L., Kinyanjui, R., Clark, J.B., Haradon, C.M., Levin, N.E., Meijer, H.J.M., Veatch, E. G., Owen, R.B., Renaut, R.W., 2018. Environmental dynamics during the onset of the Middle Stone Age in eastern Africa. Science 360, 86–90. https://doi.org/10.1126/science.aao2200.

Rao, Z., Chen, F., Cheng, H., Liu, W., Wang, G., Lai, Z., Bloemendal, J., 2013a. High-resolution summer precipitation variations in the western Chinese Loess Plateau during the last glacial. Sci. Rep. 3, 2785. https://doi.org/10.1038/srep02785.

Rao, Z., Xu, Y., Xia, D., Xie, L., Chen, F., 2013b. Variation and paleoclimatic significance of organic carbon isotopes of Ili loess in arid central Asia. Org. Geochem. 63, 56–63. https://doi.org/10.1016/j.orggeochem.2013.08.007.

Ren, J., Li, F., Chen, F., Olsen, J.W., Gao, X., 2025. Lithic technology at Banjingzi Locality 1: implications for the Middle Paleolithic in northern China. J. Archaeol. Sci. Rep 65, 105193. https://doi.org/10.1016/j.jasrep.2025.105193.

Ren, S., Song, Y., Long, H., Wu, C., Wang, Z., Yi, C., Wang, H., Zhou, L., Zheng, X., 2022. Records of organic carbon isotopic composition and its paleoenvironmental implications in Shengshan Island loess deposition in the east China sea during the last glacial period. Appl. Sci. 12, 5724. https://doi.org/10.3390/app12115724.

Ruan, J., Timmermann, A., Raia, P., Yun, K.-S., Zeller, E., Mondanaro, A., Di Febbraro, M., Lemmon, D., Castiglione, S., Melchionna, M., 2023. Climate shifts orchestrated hominin interbreeding events across Eurasia. Science 381, 699–704. https://doi.org/10.1126/science.add4459.

Sandweiss, D.H., Kelley, A.R., 2012. Archaeological contributions to climate change research: the archaeological record as a paleoclimatic and paleoenvironmental archive. Annu. Rev. Anthropol. 41, 371–391. https://doi.org/10.1146/annurev-anthro-092611-145941.

Seierstad, I.K., Abbott, P.M., Bigler, M., Blunier, T., Bourne, A.J., Brook, E., Buchardt, S. L., Buizert, C., Clausen, H.B., Cook, E., Dahl-Jensen, D., Davies, S.M., Guillevic, M., Johnsen, S.J., Pedersen, D.S., Popp, T.J., Rasmussen, S.O., Severinghaus, J.P., Svensson, A., Vinther, B.M., 2014. Consistently dated records from the Greenland GRIP, GISP2 and NGRIP ice cores for the past 104 ka reveal regional millennial-scale δ18O gradients with possible Heinrich event imprint. Quat. Sci. Rev. 106, 29–46. https://doi.org/10.1016/j.quascirev.2014.10.032.

Shang, H., Tong, H., Zhang, S., Chen, F., Trinkaus, E., 2007. An early modern human from Tianyuan Cave, Zhoukoudian, China. Proc. Natl. Acad. Sci. USA 104, 6573–6578. https://doi.org/10.1073/pnas.0702169104.

Stiner, M.C., 2013. An unshakable middle Paleolithic? Curr. Anthropol. 54, S288–S304. https://doi.org/10.1086/673285.

Tang, L., Mao, L., Shu, J., Li, C., Shen, C., Zhou, Z., 2020. Atlas of Quaternary Pollen and Spores in China. Science Press, Beijing, Springer Nature.

Tang, R.P., Ge, J.Y., Pang, H.J., Olsen, J.W., 2020. Paleohydro-climatic changes revealed by anisotropy of magnetic susceptibility at the Heitugou section, Nihewan Basin, and its influences on human's occupation. Chin. Sci. Bull. 65, 1027–1045. https://doi.org/10.1360/TB-2019-0737.

Tian, Y., Yin, Z., Zhang, X., Shao, H., Gu, M., Ren, W., Peng, C., 2022. Sedimentary characteristics and paleoenviron-mental significance of river terraces in the lower reaches of the Yixun river, Yanshan Mountains. Geol. Rev. 68, 111–121. https://doi.org/10.16509/j.georeview.2021.12.035.

Timmermann, A., 2020. Quantifying the potential causes of Neanderthal extinction: abrupt climate change versus competition and interbreeding. Quat. Sci. Rev. 238, 106331. https://doi.org/10.1016/j.quascirev.2020.106331.

Timmermann, A., Friedrich, T., 2016. Late Pleistocene climate drivers of early human migration. Nature 538, 92–95. https://doi.org/10.1038/nature19365.

Tong, H., Shang, H., Zhang, S., Chen, F., 2004. A preliminary report on the newly found Tianyuan Cave, a late Pleistocene human fossil site near Zhoukoudian. Chin. Sci. Bull. 49, 853–857. https://doi.org/10.1007/BF02889760.

Vidic, N.J., Montañez, I.P., 2004. Climatically driven glacial-interglacial variations in C3 and C4 plant proportions on the Chinese Loess Plateau. Geology 32 (2), 337. https://doi.org/10.1130/G20222.

Wang, F.X., 1995. Pollen Flora of China. Science Press, Beijing.

Wang, F., Guo, Y., Xian, Q., Li, M., Rui, X., Xie, F., 2021. Luminescence chronology for the Paleolithic site of Xinmiaozhuang Locality 1 (XMZ1) in the Nihewan Basin, northern China, and its paleoenvironmental and archaeological implications. J. Hum. Evol. 157, 103033. https://doi.org/10.1016/j.jhevol.2021.103033.

Wang, F.G., Sun, Y.C., 2023. Nihewan Archaeological Atlas. Hebei Fine Art Press, Shijiazhuang.

Wang, F.G., Yang, S.X., Ge, J.Y., Ollé, A., Zhao, K.L., Yue, J.P., Rosso, D.E., Douka, K., Guan, Y., Li, W.-., Yang, H.Y., Liu, L.Q., Xie, F., Guo, Z.T., Zhu, R.X., Deng, C.L., d'Errico, F., Petraglia, M., 2022. Innovative ochre processing and tool use in China 40,000 years ago. Nature 603, 284–289. https://doi.org/10.1038/s41586-022-04445-2.

Wang, H., Li, H., Qiu, Y., Shu, P., Liu, Y., Liu, W., Sun, J., Du, S., Wang, J., Ambrose, S.H., 2024. Seasonal landscape variability advances Lantian hominin's recognition capacity to strategically adapt to changing environments. Quat. Sci. Rev. 336, 108786. https://doi.org/10.1016/j.quascirev.2024.108786.

Wang, J., Zhou, X., Wang, S., Xu, H., Behling, H., Ye, J., Zheng, Y., Liu, J., Wu, Y., Zhao, K., Zhang, R., Li, X., 2023. C4 expansion of central Asia in the middle Miocene linked to the strengthening Indian monsoon. Global Planet. Change 224, 104096. https://doi.org/10.1016/j.gloplacha.2023.104096.

Wang, X., Chen, F., Li, F., Gao, X., 2024. Preliminary study on faunal remains unearthed from the Banjingzi Paleolithic site, Nihewan Basin, Hebei province in 2015. Huaxia Archaeol 71–79. https://doi.org/10.16143/j.cnki.1001-9928.2024.02.011.

Wang, Y., Cheng, H., Edwards, R.L., Kong, X., Shao, X., Chen, S., Wu, J., Jiang, X., Wang, X., An, Z., 2008a. Millennial- and orbital-scale changes in the east Asian monsoon over the past 224,000 years. Nature 451, 1090–1093. https://doi.org/10.1038/nature06692.

Wang, Y., Cheng, H., Edwards, R.L., Kong, X., Shao, X., Chen, S., Wu, J., Jiang, X., Wang, X., An, Z., 2008b. Millennial- and orbital-scale changes in the east Asian monsoon over the past 224,000 years. Nature 451, 1090–1093. https://doi.org/10.1038/nature06692.

Wang, Y.J., Cheng, H., Edwards, R.L., An, Z.S., Wu, J.Y., Shen, C.C., Dorale, J.A., 2001. A high-resolution absolute-dated late Pleistocene monsoon record from Hulu cave, China. Science 294, 2345–2348. https://doi.org/10.1126/science.1064618.

Wei, Q., Xie, F., 1989. Selected Treatises on Nihewan. Cultural Relics Publishing House, Beijing.

Xia, Z.K., Liu, X.Q., 1984. On paleogeography of the Nihewan basin during the accumulation of Nihewan series. Mar. Geol. Quat. Geol. 4, 101–110.

Xie, F., Li, J., Liu, L.Q., 2006. Paleolithic Archaeology in the Nihewan Basin. Huashan Literature & Arts Press, Shijiazhuang, China.

Xiong, S.F., Ding, Z.L., Liu, T.S., Zhang, J.Z., 2002. East Asian monsoon instability at the stage 4/5a transition. Boreas 31, 126–132.

Xu, J., He, X., Niu, D., Li, X., 2024. Taphonomy of the Donggou paleolithic site at Yuxian, Nihewan Basin. Acta Anthropol. Sin. 43, 1075–1090. https://doi.org/10.16359/j.1000-3193/AAS.2024.0063.

Xu, Z., Pei, S., Hu, Y., de la Torre, I., Ma, D., 2021. Stable isotope analysis of mammalian enamel from the early Pleistocene site of Madigou, Nihewan Basin: implications for reconstructing hominin paleoenvironmental adaptations in north China. Front. Earth Sci. 9, 789781. https://doi.org/10.3389/feart.2021.789781.

Xu, Z., Pei, S., Hu, Y., de la Torre, I., Ma, D., Ye, Z., Deng, C., 2023. Ecological shifts and hominin adaptations during the mid-pleistocene climate transition in northeast Asia as evidenced by isotopic analysis (δ13C, δ18O) of mammalian enamel from early paleolithic sites in the Nihewan Basin, China. Quat. Sci. Rev. 308, 108072. https://doi.org/10.1016/j.quascirev.2023.108072.

Yang, S., Ding, Z., 2014. A 249 kyr stack of eight loess grain size records from northern China documenting millennial-scale climate variability. G-cubed 15, 798–814. https://doi.org/10.1002/2013GC005113.

Yang, S., Petraglia, M.D., Hou, Y., Yue, J.P., Deng, C.L., Zhu, R.X., 2017. The lithic assemblages of Donggutuo, Nihewan Basin: knapping skills of early Pleistocene hominins in north China. PLoS One 12, e0185101. https://doi.org/10.1371/journal.pone.0185101.

Yang, S.X., Deng, C.L., Zhu, R.X., Petraglia, M.D., 2020. The Paleolithic in the Nihewan Basin, China: evolutionary history of an early to late Pleistocene record in Eastern Asia. Evol. Anthropol. Issues News Rev. 29, 125–142. https://doi.org/10.1002/evan.21813.

Yang, S.X., Wang, F.G., Xie, F., Yue, J.P., Deng, C.L., Zhu, R.X., Petraglia, M.D., 2021. Technological innovations at the onset of the mid-pleistocene climate transition in high-latitude East Asia. Natl. Sci. Rev. 8, nwaa053. https://doi.org/10.1093/nsr/nwaa053.

Yang, S.X., Zhang, J.F., Yue, J.P., Wood, R., Guo, Y.J., Wang, H., Luo, W.G., Zhang, Y., Raguin, E., Zhao, K.L., Zhang, Y.X., Huan, F.X., Hou, Y.M., Huang, W.W., Wang, Y.R., Shi, J.M., Yuan, B.Y., Ollé, A., Queffelec, A., Zhou, L.P., Deng, C.L., d'Errico, F., Petraglia, M., 2024. Initial Upper Palaeolithic material culture by 45,000 years ago at Shiyu in northern China. Nat. Ecol. Evol. 8, 552–563. https://doi.org/10.1038/s41559-023-02294-4.

Ye, Z., Pei, S., Tu, H., Du, Y., Ma, D., Li, H., Xu, J., Luo, L., Lai, Z., Granger, D., Torre, I.D. L., 2024. ^{26}Al/^{10}Be burial dating and technological strategies of hominins at the Jijiazhuang Paleolithic site, Nihewan Basin, China: Implicatiois for understanding Middle Pleistocene human adaptations in east Asia. Quat. Sci. Rev. 339, 108837. https://doi.org/10.1016/j.quascirev.2024.108837.

Yuan, B.Y., Xia, Z.K., Niu, P.S., 2011. Nihewan Rift Valley and Paleoanthropology. Geological Publishing House, Beijing.

Zan, J., Louys, J., Dennell, R., Petraglia, M., Ning, W., Fang, X., Zhang, W., Hu, Z., 2024. Mid-Pleistocene aridity and landscape shifts promoted palearctic hominin dispersals. Nat. Commun. 15, 10279. https://doi.org/10.1038/s41467-024-54767-0.

Zhang, S., Sun, Y., Li, M., Wang, N., Xu, Q., 2022a. Paleovegetation and paleotemperature in north China during the mid-Holocene based on sedimentological and palynological evidence from lake Baiyangdian. Palaeogeogr. Palaeoclimatol. Palaeoecol. 595, 110982. https://doi.org/10.1016/j.palaeo.2022.110982.

Zhang, S., Xiao, J., Xu, Q., 2022b. Regional precipitation variations during Heinrich events and dansgaard-oeschger cycles in the northern margin of the east Asian summer monsoon region. Quat. Sci. Rev. 278, 107380. https://doi.org/10.1016/j.quascirev.2022.107380.

Zhang, S., Xiao, J., Xu, Q., Wen, R., Fan, J., Huang, Y., Li, M., Liang, J., 2020. Contrasting impacts of the 8.2- and 4.2-ka abrupt climatic events on the regional vegetation of the Hulun Lake region in north-eastern China. J. Quat. Sci. 35, 831–840. https://doi.org/10.1002/jqs.3231.

Zhao, H., Lu, Y., Wang, C., Chen, J., Liu, J., Mao, H., 2010. ReOSL dating of aeolian and fluvial sediments from Nihewan basin, northern China and its environmental application. Quat. Geochronol., 12th International Conference on Luminescence and Electron Spin Resonance Dating (LED 2008) 5, 159–163. https://doi.org/10.1016/j.quageo.2009.03.008.

Zhou, S., He, X., Xu, J., Li, X., Niu, D., 2024. 2017 excavation of the Donggou paleolithic site in the Yuxian basin. Acta Anthropol. Sin. 43, 132–142. https://doi.org/10.16359/j.1000-3193/AAS.2024.0006.

Zhou, T.R., Li, H.Z., Liu, Q.S., Li, R.Q., Sun, X.P., 1991. Study on the Cenozoic Paleogeography of Nihewan Basin. Science Press, Beijing.

Zwyns, N., 2021. The Initial Upper Paleolithic in central and east Asia: blade technology, cultural transmission, and implications for human dispersals. J. Paleolit. Archaeol. 4, 19. https://doi.org/10.1007/s41982-021-00085-6.